

## Doped antiferromagnet: The instability of homogeneous magnetic phases

Assa Auerbach and B. E. Larson

*Department of Physics, Boston University, Boston, Massachusetts 02215*

(Received 18 October 1990)

The Schwinger-boson–slave-fermion mean-field theory is applied to the complete (to order  $t^2/U$ ) two-dimensional  $t$ - $J$  model at low doping and at zero temperature. A multiple Hubbard–Stratonovich transformation defines the order parameters and keeps track of their random-phase-approximation (RPA) fluctuations. The lowest mean-field state is a long-range-ordered spiral state. We find that for any  $t/J$  at infinitesimal doping, this state and other homogeneous magnetic states are unstable against local enhancement of the spiral’s pitch. The instability manifests itself at the mean-field level by a negative compressibility, and at the RPA level by negative eigenvalues of the Gaussian determinant. We discuss the implications of this instability on theory and experiments.

### I. INTRODUCTION

Recent years have seen extensive studies of the doped quantum antiferromagnet on the square lattice, and its progenitor the large- $U$  Hubbard model. These models are believed to contain some of the essential physics of the copper oxide high- $T_c$  superconductors.

The half-filled (undoped) case, which is described by the quantum Heisenberg model (QHM), is by now reasonably well understood. Theory and experiments on the high- $T_c$  related insulators (e.g.,  $\text{La}_2\text{CuO}_4$ ) are in good agreement.<sup>1</sup> The foundations of semiclassical (large- $S$ ) approaches were greatly strengthened by results of series expansions<sup>2,3</sup> and numerical simulations.<sup>4,5</sup> In addition, spin wave theory<sup>6</sup> at  $T=0$  and  $(2+1)$ -dimensional nonlinear  $\sigma$  model<sup>7</sup> have been shown to provide quantitatively reliable approximations, even for the  $S=\frac{1}{2}$  system. The large- $N$  Schwinger-boson mean-field theory<sup>8,9</sup> (SBMFT) was used to extend spin-wave theory to the disordered phase at finite temperatures. It has been found to agree with the semiclassical approaches, and to reproduce finite lattice static<sup>5,10</sup> and dynamic<sup>11</sup> correlations of the physical ( $N=2$ ) Heisenberg model. The spin correlation length of the SBMFT agrees with the one-loop order renormalization-group result of the nonlinear  $\sigma$  model.<sup>7,12</sup>

It is important to note that the projected SBMFT ground states<sup>13</sup> are total singlets which obey Marshall’s sign criterion<sup>14</sup> as required for Heisenberg antiferromagnets on bipartite lattices.

By contrast, large- $N$  mean-field theories<sup>15,16</sup> based on *fermion* representations for spins provide qualitatively different results. Their most apparent shortcoming is that their ground states cannot satisfy Marshall’s criterion.<sup>17</sup> In addition, their solutions include paramagnetic “flux phases”<sup>16</sup> and “spin-Peierls”<sup>12</sup> states, at  $T=0$ , in violation of numerical bounds for the  $N=2$ ,  $S=\frac{1}{2}$  model.<sup>4,18</sup>

The evolution of the Heisenberg antiferromagnet under slight doping  $\delta$  is microscopically described by the Hubbard model, and its projected descendant the  $t$ - $J$  model.

Three terms appear at the first two orders in  $t/U$ : the intersublattice hole hopping ( $\mathcal{H}^t$ ), the Heisenberg exchange ( $\mathcal{H}^J$ ;  $J=4t^2/U$ ), and the intrasublattice hopping term ( $\mathcal{H}^{J'}$ ), also of magnitude  $t^2/U$ . The projected electrons can be represented by Schwinger bosons and spinless fermions. This sets the problem up for a mean-field theory which extends the SBMFT to  $\delta>0$ .

In this paper we apply this mean-field theory to the three terms of the  $t$ - $J$  model, and calculate the ground-state energy for several *homogeneous* spin configurations. These include the (1,1) and (1,0) spirals, and the double spiral state.

Our main conclusion is that the homogeneous mean-field states for  $\delta>0$  are inherently *unstable*, due to the large compressibility of the holes. The system wishes to enhance the spin deviations by locally increasing the hole density. This effect is indicated by the sign reversal of the Gaussian determinant, and is signaled by a negative mean-field compressibility. Several theories<sup>19–22</sup> have predicted instability (toward phase separation) for the  $t$ - $J$  model. Here we find that the instability is robust: it appears at infinitesimal doping for all values of  $t/J$ . Since the offending fluctuations are large for all momenta below the Fermi momentum, it is unlikely that longer range Coulomb interactions could stabilize these mean-field states, although they may prevent phase separation.

Semiclassical methods<sup>23</sup> and Schwinger-boson–slave-fermion mean-field theories<sup>24–27</sup> have been previously applied to study the doped antiferromagnet. This work contains the following features.

(i) Here, the  $t$ - $J$  model includes the intrasublattice hopping term ( $\mathcal{H}^{J'}$ ) as mandated by the large  $U/t$  transformation of the Hubbard model. This term has been either ignored,<sup>24,27</sup> or replaced by an effective hopping term (called  $t'$  term) of lower symmetry.<sup>25,26</sup> The unperturbed hole band structure has a singular density of states. Our results reveal the importance of  $\mathcal{H}^{J'}$  in ruling out the canted state, and in allowing the instability of the magnetic states at infinitesimal doping.

(ii) We apply the Hubbard–Stratonovich transformation to keep track of the coupled order parameters and

their fluctuations. The ambiguity of different decompositions<sup>28</sup> of the Heisenberg interaction at low doping is resolved in Appendix A.

(iii) The unstable modes of the Gaussian matrix (i.e., the inverse RPA propagator) are identified. We reconfirm the instability of the mean-field theory for fluctuations in a range of momenta. Thus, the instability is shown to be robust.

The ordered moment in the ground state is reduced by the zero point spin wave fluctuations. A byproduct of our mean-field solution is the correlation between the ordered moment and the pitch of the spiral twist. Interestingly, we find that for the (1,1) and the (1,0) twist the ordered moment increases with the distortion.

Our mean-field results can be used to interpret the experimentally observed phase separation of  $\text{La}_2\text{CuO}_{4+\delta}$  into “oxygen-rich” and “oxygen-poor” domains.<sup>29</sup> The analysis of the RPA fluctuations indicates that the doped antiferromagnet is *highly susceptible to local deformations* in the presence of slight inhomogeneities. This may help to explain the intermediate disordered magnetic phase<sup>30</sup> in  $\text{La}_2\text{CuO}_4$  which forms at low ( $\sim 3\%$ – $5\%$ ) doping.

This work is limited to small densities of holes and small deviations from short-range antiferromagnetic order. Thus we cannot predict toward what ground state the instability leads. Two obvious possibilities are phase separation between spins and holes,<sup>19–22</sup> or the formation of local spin-hole polarons. In a planned publication<sup>31</sup> we shall use a coherent-state formulation to address this question.

The paper is organized as follows. Sections II and III are didactical; they review the derivation of the  $t$ - $J$  model from the Hubbard model, the Schwinger-bosons and slave fermions representation, and the Hubbard-

Stratonovich transformations which decouple the  $t$ - $J$  model. Although these derivations are well known to some readers, they do not often appear in the literature and are worth explaining in some detail. In particular, we expose some subtleties associated with the analytic continuation of the integration contours. Sections IV and V derive and solve the mean-field theory, Sec. VI describes the instability of the Gaussian determinant, and we end with a summary and some comments about the relevance of our results to the experimental phase diagram and to theories of high temperature superconductivity.

## II. THE $t$ - $J$ MODEL

Although there are many studies of different variants of the  $t$ - $J$  model in the literature, its full form, as derived from the large- $U$  Hubbard model is not often exposed. Here we briefly review the steps leading to the explicit form of the  $t$ - $J$  model in terms of Schwinger bosons and slave fermions.

We start with the Hubbard model, given in terms of ordinary electron operators  $c_{is}$ ,  $s = \uparrow, \downarrow$ ,

$$\mathcal{H}^{\text{Hub}} = -t \sum_{\langle i;j \rangle, s} c_{is}^\dagger c_{js} + U \sum_i \rho_{i\uparrow} \rho_{i\downarrow}, \quad (2.1)$$

where  $\langle i;j \rangle$  denotes a summation over  $i$ , and over  $z$  ( $=4$ ) nearest neighbors  $j(i)$ . Thus, there are  $z\mathcal{N}$  terms in the sum. ( $\mathcal{N}$  is the number of sites.) We define  $\rho_{is} = c_{is}^\dagger c_{is}$  and  $\rho_i = \sum_s \rho_{is}$ .

Expanding the Green's function in the nondoubly occupied subspace to second order in  $t/U$  yields the following effective Hamiltonian:

$$\begin{aligned} \mathcal{H}^U &= P_s \left[ -t \sum_{\langle i;j \rangle, s} c_{is}^\dagger c_{js} - \frac{t^2}{U} \sum_{\langle i;jk \rangle, s, s'} c_{is}^\dagger c_{js} \rho_{j\uparrow} \rho_{j\downarrow} c_{js'}^\dagger c_{ks'} \right] P_s \\ &= P_s \left[ -t \sum_{\langle i;j \rangle, s} c_{is}^\dagger c_{js} - \frac{t^2}{U} \sum_{\langle i;jk \rangle, s, s'} (c_{is}^\dagger c_{js}^\dagger c_{ks'} c_{js} + \delta_{ss'} c_{is}^\dagger c_{ks'}) \rho_j \right] P_s, \end{aligned} \quad (2.2)$$

where  $P_s \equiv \prod_i (1 - \rho_{i\uparrow} \rho_{i\downarrow})$  is the projector onto the nondoubly occupied Hilbert space. We perform the following substitutions in the second row of Eq. (2.2):

$$c_{i\uparrow} \rightarrow a_i f_i^\dagger, \quad c_{i\downarrow} \rightarrow b_i f_i^\dagger, \quad \rho_j \rightarrow f_j^\dagger f_j. \quad (2.3)$$

$a_i$  and  $b_i$  are two commuting Schwinger bosons, and  $f_i$  are spinless slave fermions. The Fock space is subject to local holonomic constraints  $P\{\cdot\}$  (a projector into the null space of  $\{\cdot\}$ ), which replaces  $P_s$

$$P_s \rightarrow P_{2S} = \prod_i P\{a_i^\dagger a_i + b_i^\dagger b_i + f_i^\dagger f_i - 2S\}. \quad (2.4)$$

Introducing the value  $2S$  (rather than the value 1) in the constraint (2.4) generalizes the  $t$ - $J$  model of  $S = \frac{1}{2}$  to arbitrary spin size. The substitutions of (2.3) in (2.2) for  $S = \frac{1}{2}$  are easily verified to yield a faithful representation of Eq.

(2.2). Thus we arrive at the form

$$\begin{aligned} \mathcal{H}^U &= P_{2S} (\mathcal{H}^t + \mathcal{H}^J + \mathcal{H}^{J'}) P_{2S}, \\ \mathcal{H}^t &= t \sum_{\langle i;j \rangle} f_i^\dagger f_j \mathcal{F}_{ij} - \mu \sum_i f_i^\dagger f_i, \\ \mathcal{H}^J &= -\frac{J}{4} \sum_{\langle i;j \rangle} \mathcal{A}_{ij}^\dagger \mathcal{A}_{ij} (1 - f_j^\dagger f_j), \\ \mathcal{H}^{J'} &= +\frac{J}{4} \sum_{\langle i;jk \rangle} f_k^\dagger f_i \mathcal{A}_{ij}^\dagger \mathcal{A}_{kj} (1 - f_j^\dagger f_j), \\ \mathcal{A}_{ij}^\dagger &\equiv (a_i^\dagger b_j^\dagger - b_i^\dagger a_j^\dagger), \quad \mathcal{F}_{ij} \equiv (a_j^\dagger a_i + b_j^\dagger b_i), \end{aligned} \quad (2.5)$$

where  $J = 4t^2/U$  is the Heisenberg superexchange constant, and we have added a chemical potential  $\mu$  for the holes. The number of terms in the summation over

$\langle i;jk \rangle$  is  $z^2\mathcal{N}$ . The notations  $\mathcal{A}_{ij}, \mathcal{F}_{ij}$  for the bilinear Bose operators are borrowed from Ref. 8.

At this point we have substituted one difficulty by another. By eliminating the large- $U$  term in the Hubbard model we have generated even more complicated interactions with local constraints. The advantage of this procedure, however, is that at half filling  $\langle f^\dagger f \rangle = \delta = 0$  all the fermion terms in (2.5) drop out, and the model reduces to the Heisenberg model<sup>8</sup> of spin  $S$ :

$$\begin{aligned} \lim_{\delta=0} \mathcal{H}^J &\rightarrow -\frac{J}{4} \sum_{\langle i;j \rangle} \mathcal{A}_{ij}^\dagger \mathcal{A}_{ij} \\ &= \frac{J}{2} \sum_{\langle i;j \rangle} (\mathbf{S}_i \cdot \mathbf{S}_j - S^2), \\ \mathbf{S}^\dagger &\equiv a^\dagger b, \quad \mathbf{S}^2 = S(S+1). \end{aligned} \quad (2.6)$$

In the following we study the partition function as given by the coherent state functional integral, with  $P_{2S}$ (2.4) imposed by Lagrange multipliers  $\lambda_i$ ,

$$Z = \int_{-\pi}^{\pi} d\lambda \int \mathcal{D}\{a^\dagger ab^\dagger b f^\dagger f\} \exp \left[ \int_0^\beta d\tau \sum_i (a_i^\dagger \dot{a}_i + b_i^\dagger \dot{b}_i + f_i^\dagger \dot{f}_i) - \mathcal{H}^J + i \sum_i \lambda_i (a_i^\dagger a_i + b_i^\dagger b_i + f_i^\dagger f_i - 2S) \right]. \quad (2.7)$$

### III. THE HUBBARD-STRATONOVICH TRANSFORMATIONS

In this section we introduce Hubbard-Stratonovich (HS) transformations which decouple the four- and six-operator terms in  $\mathcal{H}^J$ , Eq. (2.5). The basic identity is just that of a Gaussian integral. For any Hermitian interaction between operators  $\mathcal{B}$  and  $\mathcal{C}$  (which could be labeled by time and spatial indices) one has the identity

$$\exp[g(\mathcal{B}^\dagger \mathcal{C} + \mathcal{C}^\dagger \mathcal{B})] = \frac{1}{(2\pi)^2} \int_{-\infty}^{\infty} d\Lambda_1^b d\Lambda_2^b d\Lambda_1^c d\Lambda_2^c \exp \left[ - \left[ \mathcal{B}^\dagger C + B \bar{C} + \mathcal{C}^\dagger B + C \bar{B} + \frac{\bar{B}C + \bar{C}B}{g} \right] \right], \quad (3.1)$$

where the integration is over four *real* fields  $\Lambda_\alpha^{(b,c)}$ ,  $\alpha=1,2$ . Without loss of generality we can choose  $g > 0$ . (A negative sign could be absorbed in, say,  $\mathcal{B}$ .) The complex fields  $B, C$  and their bars are defined by

$$\begin{aligned} B(C) &\equiv \Lambda_1^{b(c)} + i\Lambda_2^{b(c)}, \\ \bar{B} &\equiv \Lambda_1^c - i\Lambda_2^c, \\ \bar{C} &\equiv \Lambda_1^b - i\Lambda_2^b. \end{aligned} \quad (3.2)$$

The definition of the ‘‘barred’’ fields might seem puzzling: they are not related in any way to their unbarred counterparts. The definitions (3.2), however, are natural for the mean-field theory. We shall see that in order to allow  $B$  and  $C$  to be independent complex parameters we must deform the contours of integration in (3.1) into the complex plane. We shall return to this important point later. The real fields  $\Lambda_\mu^\alpha$ ,  $\mu=1,2$ ,  $\alpha=b,c$ , must be used for the Gaussian integration in the RPA theory.

In Eq. (2.5) there are terms up to eighth order in the Bose and Fermi operators. As a first simplification, we replace the hole density  $f_j^\dagger f_j \rightarrow \delta$  in  $\mathcal{H}^J$  and  $\mathcal{H}^J$ , and define  $J_\delta = J(1-\delta)$ . This substitution neglects hole correlation corrections which are higher order in  $\delta$ . By applying the HS identity (3.1) to (2.7) once, we can replace the Heisenberg terms in (2.5) at each time by

$$\mathcal{H}^J \rightarrow \sum_{\langle i;j \rangle} \left[ \mathcal{A}_{ij} Q_{ij}^* + \mathcal{A}_{ij}^\dagger Q_{ij} + \frac{4|Q_{ij}|^2}{J_\delta} \right]. \quad (3.3)$$

$Q$  is precisely the field which serves as the ‘‘order parameter’’ in the Schwinger-boson mean-field theory of the pure Heisenberg model.<sup>8</sup> In Appendix A we show why, at low doping, the other ‘‘ferromagnetic’’ decomposition<sup>28</sup> need not be considered. The  $\mathcal{H}^J$  terms are decoupled by

$$\begin{aligned} \mathcal{H}^J &\rightarrow \sum_{\langle i;j \rangle} \left[ f_i^\dagger f_j F_{ij} + (a_j^\dagger a_i + b_j^\dagger b_i) \bar{T}_{ij} - \frac{\bar{T}_{ij} F_{ij}}{t} \right], \\ F_{ij} &= \bar{F}_{ji}, \quad \bar{T}_{ij} = T_{ji}. \end{aligned} \quad (3.4)$$

The intrasublattice hopping terms of  $\mathcal{H}^J$  are enumerated by triads of lattice indices  $\langle i;jk \rangle$ . Since they are of sixth order, we apply the transformation (3.1) twice successively to yield

$$\begin{aligned} \mathcal{H}^J &\rightarrow \sum_{\langle i;jk \rangle} f_k^\dagger f_i \bar{K}_{ijk} + \mathcal{A}_{ij}^\dagger N_{ij}^k + \mathcal{A}_{jk} \bar{N}_{jk}^i \\ &\quad - \frac{N_{ij}^k \bar{N}_{jk}^i}{M_{ijk}} - \frac{4M_{ijk} \bar{K}_{ijk}}{J_\delta}, \end{aligned} \quad (3.5)$$

where the fields are taken to obey  $O_{ijk} = \bar{O}_{kji}$ . At this point we have decoupled all the interactions and separated the bosons from the fermions, leaving us only with bilinear terms [Eqs. (3.3)–(3.5)]. In the following we shall apply the steepest descents method (i.e., the mean-field approximation) to evaluate the ground-state energy of  $\mathcal{H}^J$ .

### IV. THE MEAN-FIELD THEORY

The mean-field theory is given by replacing all the HS fields and the constraints field  $\lambda$  by static variational parameters. In order for the bilinear Hamiltonian to be Hermitian [see (3.1)] we require that all saddle-point fields obey

$$\bar{B}_{\text{MF}} = (B_{\text{MF}})^*; \quad B = F, T, N, M, K, Q. \quad (4.1)$$

At first sight, the definitions (3.2) and the requirement (4.1) seem to imply that  $B_{\text{MF}}$  is equal to  $C_{\text{MF}}$ . This re-

striction is circumvented by analytical continuation of both  $\Lambda_1^{(b,c)}$  and  $\Lambda_2^{(b,c)}$  into the complex plane where the true saddle point is situated. This scenario is analogous to allowing the constraint field  $\lambda$  to be purely imaginary at the saddle point. The integration contour enters the calculation of the Gaussian fluctuations<sup>32,8</sup> (see Sec. VI).

The mean-field ground state depends on the magnitude and symmetry of the mean-field parameters which act as driving fields. As in standard Hartree-Fock decompositions the mean-field equations, through minimizing the energy, relate the *fields* to the *correlations*,

$$\begin{aligned} Q_{ij} &= \frac{J_\delta}{4} \langle \mathcal{A}_{ij} \rangle, \quad F_{ij} = t \langle \mathcal{F}_{ij} \rangle, \\ T_{ij} &= t \langle f_i^\dagger f_j \rangle, \\ K_{ijk} &= \frac{J_\delta}{4} \langle \mathcal{A}_{ij} \mathcal{A}_{kj}^\dagger \rangle, \quad \text{etc., . . .} \end{aligned} \quad (4.2)$$

Equations (4.2) can hold only if the symmetries of the correlations are identical to the symmetries of the driving fields. Consequently,  $T_{ij}$  and  $F_{ij}$  have the same symmetry.

- 
- (a) (1,0) spiral:  $\hat{F}_{\hat{\eta}} = \frac{1}{\sqrt{2}}(1, -1, 0, 0)$ ,  $\hat{F}_{\mathbf{k}} = i[\sqrt{2} \sin(k_x)]$ ,  
 (b) (1,1) spiral:  $\hat{F}_{\hat{\eta}} = \frac{1}{2}(1, -1, 1, -1)$ ,  $\hat{F}_{\mathbf{k}} = i[\sin(k_x) + \sin(k_y)]$ ,  
 (c) (1, $i$ ) spiral:  $\hat{F}_{\hat{\eta}} = \frac{1}{2}(1, -1, i, -i)$ ,  $\hat{F}_{\mathbf{k}} = i[\sin(k_x) + i \sin(k_y)]$ ,  
 (d) canted state:  $\hat{F}_{\hat{\eta}} = \frac{1}{2}(1, 1, 1, 1)$ ,  $\hat{F}_{\mathbf{k}} = 2\gamma_{\mathbf{k}}$ ,

where  $\hat{F}_{\mathbf{k}} = \sum_{\hat{\eta}} e^{ik \cdot \hat{\eta}} \hat{F}_{\hat{\eta}}$  and  $\gamma_{\mathbf{k}} = (1/4) \sum_{\hat{\eta}} e^{ik \cdot \hat{\eta}}$ . Cases (a) and (b) represent spiraling coplanar spins, case (c) represents spiraling in two perpendicular planes in the  $x$  and  $y$  directions (“double spiral”). This state cannot be realized classically on an infinite planar lattice. The ordered moment that will emerge, at  $T=0$ , is taken to be an artifact of softening the constraint in the mean-field theory. Case (d) represents a nonzero uniform magnetization due to the canting of one sublattice’s magnetization relative to the other.

From (4.3) we learn that  $\langle \mathcal{A} \rangle$  depends only *quadratically* on small distortions  $\langle \mathcal{F} \rangle$ ; a fact which can be verified from the mean-field solutions. Thus the symmetry of the related fields  $Q, K, N, M$  remains unchanged by the doping. We take them all to be real and uniform constants.<sup>33</sup>

Substituting the dynamical fields in (3.3)–(3.5) by (4.4), and diagonalizing the mean-field Hamiltonian leads to the energy function

$$\begin{aligned} E[\Lambda^\alpha] &= \sum_{\mathbf{k}\pm}^{\text{red}} \omega_{\mathbf{k}}^\pm + \sum_{\mathbf{k}\pm}^{\text{red}} \epsilon_{\mathbf{k}}^\pm f(\epsilon_{\mathbf{k}}^\pm) + \frac{zQ^2}{J_\delta} - 4z^2 \frac{MK}{J_\delta} \\ &\quad - z^2 \frac{N^2}{M} - \frac{FT}{t} - \lambda(2S + 1 - \delta). \end{aligned} \quad (4.5)$$

Here the fermion filling is  $\sum_{\mathbf{k}\pm}^{\text{red}} f(\epsilon_{\mathbf{k}}^\pm) = \delta$ , and  $\sum^{\text{red}}$  denotes a sum over the reduced Brillouin zone. The fermion bands are given by

The unfortunate property of  $SU(N)$  mean-field theories is that the bilinear operators such as  $\mathcal{A}$  and  $\mathcal{F}$  do not directly represent spin operators since they violate the constraint. They should rather be thought of as “square roots” of legitimate spin operators as seen in the following identities:

$$\frac{1}{2} \mathcal{A}_{ij}^\dagger \mathcal{A}_{ij} = (\mathbf{S}_i - \mathbf{S}_j)^2, \quad \frac{1}{2} \mathcal{F}_{ij}^\dagger \mathcal{F}_{ij} = (\mathbf{S}_i + \mathbf{S}_j)^2, \quad (4.3)$$

where  $::$  indicates normal ordering. Equation (4.3) allows us to interpret the *magnitude* of the fields  $Q_{ij}$  ( $F_{ij}$ ) as the difference (sum) of neighboring spins. There is additional information in the *phases* of the  $Q$  and  $F$  fields, which has been exposed by Kane *et al.*<sup>25</sup> They have found that for  $|F| \ll |Q|$  (neighboring spins nearly antiparallel), the gauge-invariant content of the phases corresponds to the relative directions of the spins on the two sublattices. Specifically, they have classified four different symmetries of the homogeneous spin states using the symmetry of the vector  $\hat{F}_{i,i+\hat{\eta}}$  where  $i$  is on one sublattice, and  $\hat{\eta} = \pm\hat{x}, \pm\hat{y}$ . Defining  $F_{i,i+\hat{\eta}} \equiv F \hat{F}_{\hat{\eta}}$  and  $T_{i,i+\hat{\eta}} \equiv T \hat{F}_{\hat{\eta}}$ , the cases are

---


$$\epsilon_{\mathbf{k}}^\pm = z^2 K \gamma_{\mathbf{k}}^2 \pm F |\hat{F}_{\mathbf{k}}|. \quad (4.6)$$

It is important to note that the fermion band structure, in the absence of doping, is a special one. For  $F=0$  the minima lie on the line  $\gamma_{\mathbf{k}}=0$ , and the density of states  $\rho^0$  has a singularity of

$$\rho^0(\epsilon) \simeq \epsilon^{-1/2} |\ln(\epsilon)|. \quad (4.7)$$

This is the result of a degeneracy between different next-neighbor hopping matrix elements in  $\mathcal{H}'$ . This singularity distinguishes this band structure from that obtained by fermion self-energy corrections.<sup>34</sup> In Fig. 1 we plot the lowest band  $\epsilon_{\mathbf{k}}^-$ , and the occupied Fermi volume for the (1,0) and (1,1) spirals. The (1, $i$ ) and the (1,0) cases have similar band structures. As the reader can see, the Fermi surfaces are highly elliptical, and are located in a region of highly density of states.

The band structure (4.6) rules out the canted state [case d, Eq. (4.4)], since the distortion  $F$  couples to the fermion band with a vanishing weight  $\gamma_{\mathbf{k}} \simeq 0$  near the minima of the unperturbed bands. This results in a quadratic dependence of the fermion energy on  $F$  and does not allow a nonzero solution for  $T$  and  $F$  at small values of  $\delta$ . The canted state at low doping can only emerge if  $\mathcal{H}'$  is ignored, as in Ref. 24.

The Bose dispersions, for the spiral cases, are

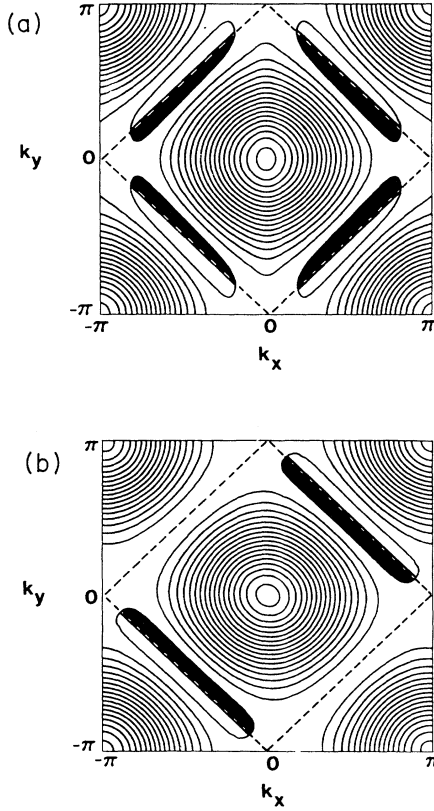


FIG. 1. The lower hole band  $\epsilon_{\mathbf{k}}^-$ , [Eq. (4.6)], for (a) the (1,0) spiral state and (b) the (1,1) spiral state. The (1, $i$ ) double spiral state has a similar band structure to (a). The dark regions are occupied states within the reduced Brillouin zone.

$$\omega_{\mathbf{k}}^{\pm} = \sqrt{(\lambda \pm T |\hat{F}_{\mathbf{k}}|)^2 - (Q + 2zN)^2 (z\gamma_{\mathbf{k}})^2} \geq 0. \quad (4.8)$$

In Fig. 2 we plot the spin wave dispersions  $\omega_{\mathbf{k}}^{\pm}$  along a line which contains the zeros of  $\omega_{\mathbf{k}}^-$  which are at  $\pm \mathbf{k}_t$ . When Bose condensation occurs<sup>35</sup> (at zero temperature for all  $S > S_c \approx 0.2$ ),  $\langle S^+(\mathbf{x}) \rangle = m_0 e^{ik_t x}$ , which identifies  $\mathbf{k}_t$  as the pitch of the spiral.

The mean-field equations are generated by setting  $\partial E^{\text{MF}} / \partial \Lambda^{\alpha} = 0$  ( $\alpha$  runs over all the HS fields). First we eliminate the parameters of  $H^J$  by differentiating  $E$  with respect to  $\Lambda = Q, N, M, K$ , yielding

$$2Q/J_{\delta} = -N/M = -2\sqrt{K/J_{\delta}} \quad (4.9)$$

and

$$M/J_{\delta} = \frac{1}{4} \sum_{\mathbf{k}^{\pm}} \gamma_{\mathbf{k}}^2 f(\epsilon_{\mathbf{k}}^{\pm}) = -\alpha \delta^3, \quad \alpha = O(1). \quad (4.10)$$

Equations (4.9) and (4.10) allow us to substitute the fermion intrasublattice hopping  $K$  by the value  $Q^2/J_{\delta}$ . We wish to retain energies up to quadratic order in  $\delta$ . Using (4.9) and (4.10) to substitute  $N$  in (4.8), one gets  $Q + 2zN = Q(1 - 2z\alpha\delta^3) \approx Q$ , which allows us to discard this weak “feedback” effects of  $H^J$  on the spin wave velocity. Thus,  $K$ ,  $M$ , and  $N$  have been eliminated from the

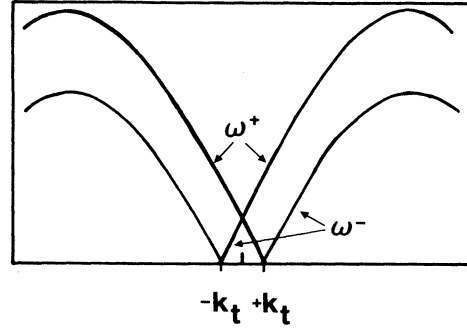


FIG. 2. The Schwinger boson dispersions  $\omega_{\mathbf{k}}^{\pm}$  [Eq. (4.8)], in the spiral states along the direction of the ordering wave vector  $\mathbf{k}_t$ .  $\mathbf{k}_t$  measures the pitch of the spiral (see text).

mean-field equations.

The remaining equations are

1. The constraint equation

$$\sum_{\mathbf{k}^{\pm}}^{\text{red}} \frac{\partial \omega_{\mathbf{k}}^{\pm}}{\partial \lambda} = \sum_{\mathbf{k}^{\pm}}^{\text{red}} \frac{\lambda \pm T |\hat{F}_{\mathbf{k}}|}{\sqrt{(\lambda \pm T |\hat{F}_{\mathbf{k}}|)^2 - Q^2 (z\gamma_{\mathbf{k}})^2}} = 2S + 1 - \delta, \quad (4.11)$$

which determines the ordered moment  $m_0$ , given a twisting force  $T$ .

2. The spin-wave velocity equation

$$\sum_{\mathbf{k}^{\pm}}^{\text{red}} \frac{\partial \omega_{\mathbf{k}}^{\pm}}{\partial Q} = \sum_{\mathbf{k}^{\pm}}^{\text{red}} \frac{-Qz^2\gamma_{\mathbf{k}}^2}{\sqrt{(\lambda \pm T |\hat{F}_{\mathbf{k}}|)^2 - (zQ\gamma_{\mathbf{k}})^2}} = -2zQ/J_{\delta}, \quad (4.12)$$

determines the value of the spin wave velocity  $c = zQ/\sqrt{2}$  as a function of the driving field  $T$ .

3. The pitch equation

$$\sum_{\mathbf{k}^{\pm}}^{\text{red}} \frac{\partial \omega_{\mathbf{k}}^{\pm}}{\partial T} = \sum_{\mathbf{k}^{\pm}}^{\text{red}} \frac{\pm |\hat{F}_{\mathbf{k}}| (\lambda \pm T |\hat{F}_{\mathbf{k}}|)}{\sqrt{(\lambda \pm T |\hat{F}_{\mathbf{k}}|)^2 - (zQ\gamma_{\mathbf{k}})^2}} = F/t, \quad (4.13)$$

relates the twisting force  $T$  to the induced spin correlation  $F$ .

4. The fermion twisting force equation

$$\sum_{\mathbf{k}, \pm; \epsilon_{\mathbf{k}}^{\pm} \leq \mu} \pm \hat{F}_{\mathbf{k}} = T/t. \quad (4.14)$$

Using Eqs. (4.9), (4.11)–(4.14), we find (see Appendix B) the mean-field energy to be simply given by

$$E^{\text{MF}} = \frac{TF}{t} - \frac{zQ^2}{J_{\delta}}. \quad (4.15)$$

Here  $T, F, Q$  are completely determined by the microscopic parameters  $t, J, S$ , and  $\delta$ .

#### A. Slave fermions and magnetic band-structure electrons

The spin density wave (SDW) Hartree-Fock approximation of the Hubbard model, Eq. (2.1) involves substi-

tuting

$$U\rho_{i\uparrow}\rho_{i\downarrow} \rightarrow U(\rho_{i\uparrow} + \rho_{i\downarrow})m_0 e^{i\pi i} - Um_0^2, \quad (4.16)$$

where  $m_0$  is the staggered magnetization per site. Equation (4.16) yields the “magnetic band structure” for the electrons

$$\begin{aligned} \epsilon_k^{\text{SDW}} &= \pm \sqrt{(m_0 U)^2 + (zt\gamma_k)^2} \\ &= \pm \left[ m_0 U + \frac{z^2 t^2 \gamma_k^2}{2Um_0} + O(t^4/U^2) \right]. \end{aligned} \quad (4.17)$$

At half filling, the lower band is filled, and the upper band is empty. If we take the large- $U$  limit of (4.17) and substitute  $m_0 \rightarrow \frac{1}{2}$ , the lower (hole) band can be mapped onto the undistorted ( $F=0$ ) slave fermion bands:

$$\epsilon_k^\pm = K(S = \frac{1}{2})(z\gamma_k)^2 \rightarrow Jz^2\gamma_k^2 \approx \epsilon_k^{\text{SDW}} + m_0 U. \quad (4.18)$$

The substitution of  $K$  in (4.18) by  $JS^2$  is justified in the semiclassical limit (large  $S$ ) since by (4.9)  $K = Q^2/J$ , and from Ref. 9  $Q = (1 + 0.078974/S)JS$ .

Thus, the fermion quasiparticles in the Néel state are similar in the two approaches. They have similar dispersions and are restricted to hopping only on the same sublattice. This relates the weak coupling approximation to the Hubbard model, to the large- $U$   $t$ - $J$  model limit. The major distinction between the two theories is that the slave fermions are described in a *rotationally invariant formulation* which does not require long-range order. The slave fermion dispersions also incorporate the quantum effects of the spin waves.

## V. RESULTS OF THE MEAN-FIELD THEORY

In Appendix B we solve Eqs. (4.11)–(4.14) in detail and derive the mean-field ground-state energy, compressibility, and the ordered moment to second order in the doping concentration  $\delta$ . We find that the (1,1) spiral is lowest in energy for  $S < 0.81$ , while the (1,0) spiral wins for larger spin sizes. The mean-field energy is given by

$$E^{\text{MF}} = -4JZ_c^2 S^2 + 4Z_1 JS^2 \delta + \frac{1}{2} \kappa \delta^2, \quad (5.1)$$

$$Z_c = 1 + \frac{0.078974}{S}, \quad Z_1 = Z_c^2 \left[ \left( 1 + \frac{1}{S} \right) - \frac{dZ_c}{dS} \right].$$

$E^{\text{MF}}$  is plotted in Fig. 3 for  $S = \frac{1}{2}$  and  $t/J = 2$ . It is important to note that the linear (chemical potential) term  $4Z_1 JS^2$  in Eq. (5.1) does not depend on  $t$  at all.  $\kappa(S, t, J)$  is the compressibility, given by

$$\kappa(S) = -2JS^2 \left[ \left( \frac{t}{J} \right)^2 A(S) + \frac{4}{S} Z_c + \frac{1}{S^2} \right]. \quad (5.2)$$

The values of  $A(S)$  for the (1,1) and (1,0) spirals are given in Eq. (B8). For  $S = \frac{1}{2}$ , we find that  $4Z_c^2 = 5.36$ , and  $4Z_1 = 14.36$ , while

$$\kappa_{1/2} = \begin{cases} -25.76 & (1,0) \text{ spiral} \\ -44.16 & (1,1) \text{ spiral} \\ -0.99 & (1,i) \text{ spiral} \end{cases}. \quad (5.3)$$

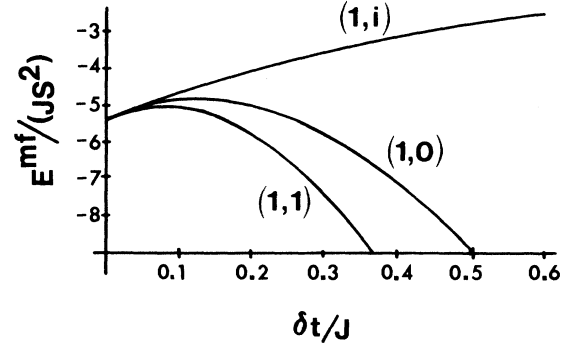


FIG. 3. The mean-field energy vs density  $\delta$  for three spiral states labeled by the direction of the twist. The plot is for  $S = \frac{1}{2}$  and  $t/J = 2$ .

The terms which depend on the symmetry of the spiral are of order  $\delta^2$  and higher. Therefore  $\kappa$  determines the lowest state, which for  $S = \frac{1}{2}$  is the (1,1) spiral.

The negativity of  $\kappa$  for all values of  $t/J$  and  $S$  is the most important fact about the mean-field energy. The origin of this effect could be traced back to two effects. (1) The  $(1-\delta)^2$  renormalization of the Heisenberg energy due to reduction of the spins and (2) the coupling to the Fermion energy which is linear in the hole density. The negative  $\kappa$  suggests the possibility of phase separation<sup>19–22</sup> between a hole-rich phase and the Néel phase, it provided the energy function is minimized by homogeneous states at large doping. Alternatively, the system can form local defects or spin polarons, which will describe the quasiparticles of a new phase.

The positivity of the linear term in (5.1) implies that the untwisted Néel state is metastable, and would suffer a *first-order transition* toward the true ground state.

A byproduct of this calculation is the correlation between the Bose-condensed fraction, or ordered moment<sup>35</sup>  $m_0$  and the pitch of the spiral  $k_t$ , which define the spin directions in the ground state by

$$\langle S^x(\mathbf{x}) + iS^y(\mathbf{x}) \rangle = m_0 e^{ik_t \cdot \mathbf{x}}. \quad (5.4)$$

In Fig. 4, this correlation is depicted for the three spiral states. It is interesting to note that the moment *increases* as the spins are twisted (without doping) in the (1,0) and (1,1) direction. The double spiral, however, rapidly loses its Bose condensation.

## VI. INSTABILITY OF THE RPA THEORY

Here we strengthen the case for the instability of the mean-field states by calculating the fluctuations of the HS fields at low doping. The partition function (2.7) is expanded about its saddle point to Gaussian order:

$$Z^{(2)} \approx \exp(-\beta E^{\text{MF}}) \int \mathcal{D}[\Lambda] \exp(-\Lambda^\dagger \Pi \Lambda). \quad (6.1)$$

Here we use the notation of Eq. (3.1):

$$\Lambda = \Lambda_{\mu}^{\alpha}(i, \hat{\eta}, \omega),$$

$$\alpha = Q, F, T, N, M, K, \quad \mu = 1, 2, \quad (6.2)$$

and

$$\alpha = \lambda, \mu = 1,$$

where  $\Lambda_{\mu}^{\alpha}$  are integrated over the real axis as in Eq. (3.1). Let us concentrate on the submatrix  $\Pi^{t,f}$  in the  $T, F$  subspace, which determines the quadratic form

$$\Lambda^{\dagger} \Pi^{t,f} \Lambda = \sum_{\mu=1,2} (\Lambda_{\mu}^t, \Lambda_{\mu}^f) \begin{pmatrix} \frac{1}{t} \delta_{i\hat{\eta}, i'\hat{\eta}'} & -\chi^b(i\hat{\eta}, i'\hat{\eta}') \\ -\chi^f(i\hat{\eta}, i'\hat{\eta}') & \frac{1}{t} \delta_{i\hat{\eta}, i'\hat{\eta}'} \end{pmatrix} \begin{pmatrix} \Lambda_{\mu}^t \\ \Lambda_{\mu}^f \end{pmatrix}, \quad (6.3)$$

where  $\chi^b$  and  $\chi^f$  are the dynamical susceptibilities of the bosons and fermions with respect to the twist fields  $T$  and  $F$ , respectively. The determinant is thus

$$\det|\Pi^{\text{TF}}| = (1/t)^2 - \chi^b \chi^f. \quad (6.4)$$

At momenta smaller than the Fermi momentum, the Fermi and Bose susceptibilities can be estimated as being close to their long wavelength limit

$$\chi^f = \rho(\mu) |\hat{F}_{k_0}|^2 [1 + O(q/k_f)] \approx \frac{1}{\pi t \sqrt{\delta}},$$

$$\chi^b \approx \frac{(S - S_c)}{JS}. \quad (6.5)$$

Since the fermion density of states increases significantly for small  $\delta$ , the determinant of (6.4) becomes *negative* for any value of  $t/J$ . This clearly identifies the unstable modes as the correlated hole density-spin twist fluctuations.

The matrix elements which connect the  $F$  and  $T$  fields to the other HS fields, such as  $Q$ ,  $\lambda$ ,  $K$ ,  $M$ , and  $N$ , are all of order  $F \sim T \sim \delta$ , because, by symmetry, the cross susceptibilities vanish in the undistorted  $F=0$  limit. Thus they will only effect Eq. (6.4) by corrections of order  $\delta^2$ .

This result is robust against the following changes in our microscopic model.

(i) Additional hopping terms will not enable (6.4) to be positive unless they drastically reduce the fermion density of states, and if  $t/J$  is not large. The  $t < J$  regime, however, is not derivable from the large- $U$  Hubbard model.

(ii) Long-range Coulomb forces will stabilize against macroscopic phase separation by screening the  $q=0$  instability. In the slightly doped antiferromagnet, however, it is hard to see how this screening could be effective at wavelengths of the order of the interparticle separation.

## VII. SUMMARY AND FUTURE DIRECTIONS

We have found that the homogeneous spiral states, which solve the mean-field theory of the  $t$ - $J$  model close to half filling, are inherently unstable. Since our approach is limited to small distortions about the Néel configuration, it cannot determine the thermodynamic ground state. For larger distortions, the present approximation scheme becomes more involved; the relative

effects of the  $t$  and  $J$  hopping terms change, and more possible mean-field decompositions need to be considered for each interaction (see Appendix A).

There are experimental and theoretical implications of this instability. Recent experiments<sup>29</sup> in high pressure oxygenated  $\text{La}_2\text{CuO}_4$  have observed phase separation into oxygen-rich and oxygen-poor domains. It is known that the hole concentration in the copper-oxide planes is proportional to the oxygen concentration. The fact that the transition occurs at around the Néel temperature suggests that the oxygen phase separation may be driven by the negative in-plane hole compressibility.

In Sec. VI we have identified the unstable modes as those associated with coupled spin-hole fluctuations. This suggests that the nearly pure antiferromagnet is highly susceptible to local charge perturbations which couple to the spin distortions and break the translational invariance of the ground state.

One class of theories of high temperature superconductivity<sup>36-38</sup> involves a model which resembles the  $t$ - $J$  model (2.5) but where the effects of the intersublattice hopping  $\mathcal{H}^t$  are ignored. The pairing occurs via the intrasublattice hopping which is coupled to the spin fluctuations through a gauge field. This coupling can be *microscopically* derived directly from  $\mathcal{H}^f$  in Eq. (2.5). However, the pairing requires<sup>38</sup> no longer-range order, and massive Schwinger bosons at zero temperature. Here we found that the long-range order did *not* vanish in the mean-field states, and that the  $t$  term was important. However, since the spiral states are unstable, the possibility of local spin-polaron type quasiparticles emerges. In a forthcoming publication we shall study the properties of spin polarons,<sup>31</sup> and find that they can hop only on one sublattice. Perhaps, one might speculate, the spin polarons form a band of weakly interacting quasiparticles for which the gauge field pairing mechanism is applicable. A more traditional point of view is that the spin-hole bound states reincarnate the electronlike Fermi liquid excitations.

## ACKNOWLEDGMENTS

We thank the authors of Ref. 25 for sending us their manuscript prior to publication, and B. I. Halperin for a discussion on RPA stability. This work has been supported by the National Science Foundation (NSF), Grant

No. DMR-891045. A. Auerbach acknowledges the Alfred P. Sloan Foundation for support.

#### APPENDIX A: WHY WE CONSIDER ONLY ONE DECOUPLING POSSIBILITY

The decomposition of Eq. (3.3) is not unique; it is possible to write

$$\mathcal{H}^J = -\frac{(J-J_1)}{4} \sum_{\langle i;j \rangle} \mathcal{A}_{ij}^\dagger \mathcal{A}_{ij} + \frac{J_1}{4} \sum_{\langle i;j \rangle} (\mathcal{F}_{ij}^\dagger \mathcal{F}_{ij}) - J_1 z S^2, \quad (\text{A1})$$

where  $\mathcal{A}_{ij}$  and  $\mathcal{F}_{ij}$  are the antiferromagnetic and ferromagnetic bilinear forms, respectively. [See Eq. (2.5) for their definitions.] In principle both terms could be decomposed separately, as was done<sup>28</sup> in Ref. 25. However, to fully minimize the energy,  $J_1$ , which is a *free parameter* in the range  $[0, J]$ , needs to be determined variationally. Here we carry out this procedure to low order in  $\delta$ . First, the two terms of (A1) are decoupled using the fields  $Q$  and  $F$ , respectively, yielding a mean-field equation for the value of  $F$ :

$$\frac{\partial E}{\partial F} \approx -4z^2 \chi_F F - zF/J_1, \quad (\text{A2})$$

which  $\chi$  is essentially the ferromagnetic susceptibility (modulo a weak dependence on the symmetry of the  $F$  field), and is of the order of  $1/[2z(J-J_1)]$ . It is therefore clear that Eq. (A2) cannot be satisfied for small  $J_1 \ll J/2$  unless  $F=0$ . The ground-state energy at  $\delta=0$  is given by

$$E = -\frac{zQ^2}{(J-J_1)} + \frac{zF^2}{J_1} - zJ_1 S^2. \quad (\text{A3})$$

From the results of the SBMFT (Ref. 9) we know that

$$Q(F=0) = Z_c (J-J_1) S > (J-J_1) S, \quad (\text{A4})$$

since the quantum correction to  $Z_c$  is positive.<sup>9</sup> Therefore from (A3) we find that

$$E(J_1) > E(J_1=0). \quad (\text{A5})$$

The discussion given above also holds in the presence of small amount of doping. There a driving field  $T = -t\delta$  due to the fermions adds to  $F$ . Since  $\chi_F$  changes only by order  $T$ , Eq. (A2) would still not enable a nonzero solution for  $F$ , and the previous conclusion about  $J_1$  holds.

These arguments, however, do not hold for  $\delta = O(1)$ . Then the fields  $Q$ ,  $T$ , and therefore  $\chi_F$ , significantly differ from the pure case, and competing decompositions, as in Eq. (A1), should be considered.

#### APPENDIX B: THE SOLUTION OF THE MEAN-FIELD EQUATIONS

The four coupled equations are solved for small value of the driving fields  $T$  and  $F$ . First we examine the effect of the twist  $F$  on the fermion band structure: when  $F_{\mathbf{k}}$  is subtracted from the Néel bands, it creates elliptical pock-

ets in the lower band  $\epsilon_{\mathbf{k}}^-$  centered at  $k_0 = (\pm\pi/2, \pm\pi/2)$ , for the (1,0) and (1, $i$ ) cases, and  $k_0 = \pm(\pi/2, \pi/2)$  for the (1,1) case. See Fig. 1. The Fermi energy is given by

$$\mu = -|F_{k_0}| \delta / \rho, \quad \rho = \frac{1}{\pi z S \sqrt{J_\delta |F_{k_0}|}}. \quad (\text{B1})$$

We assume here, and will confirm later, that  $F_{k_0} \geq O(\delta)$ . Thus, by (B1), the Fermi energy is approximately  $-|F_{k_0}|$ . Hence, all the fermions spill into the pockets of the lower bands, thereby simplifying the mean-field equation (4.14) considerably:

$$T = -t \delta \hat{F}_{k_0}. \quad (\text{B2})$$

The importance of Eq. (B2) is that it establishes that the driving field for the twist  $T$  is of order  $\delta$ , and therefore could be made arbitrarily small.

Since the left-hand side of the pitch equation (4.13) is linear in  $T$ , we verify our previous assumption that  $F \propto \delta$ .

Combining Eqs. (4.9), (4.11)–(4.14), and (B2), we arrive at a simplified form of the mean-field energy of the  $t$ - $J$  model (4.5):

$$E^{\text{MF}} = \frac{TF}{t} - \frac{zQ^2}{J_\delta}. \quad (\text{B3})$$

The values of  $\lambda/c$  are fixed by requiring  $\omega_{\mathbf{k}}^\pm$  to vanish at some pitch wave vector  $\mathbf{k}_t$ . This is a necessary condition for satisfying the constraint equation (4.11) in the ordered phase at  $S > S_c \approx 0.2$ . The symmetry of the spirals together with the form of  $\omega_{\mathbf{k}}^\pm$  shows that solutions of  $\omega_{\mathbf{k}}^\pm = 0$  must correspond to  $k$  vectors  $\pm(k_t, 0)$ ,  $\pm(k_t, k_t)$ , and  $\pm(k_t, \sigma k_t)$  (with  $\sigma = \pm 1$ ) for the (1,0), (1,1), and (1, $i$ ) spirals, respectively. Since  $\omega_{\mathbf{k}}^\pm$  must be positive semidefinite  $\omega_{\mathbf{k}}^{\pm 2} = 0$  has a double root. This observation allows  $k_t$  and  $\lambda/c$  to be found, the latter from the condition of vanishing discriminant, yielding

$$k_t = \begin{cases} \cos^{-1}[1+8(T/c)^2]^{-1/2} & (1,0), (1,1) \text{ spirals}, \\ \cos^{-1}[1+4(T/c)^2]^{-1/2} & (1,i) \text{ spiral}, \end{cases} \quad (\text{B4})$$

$$\lambda/c = \begin{cases} (1+\sqrt{1+8(T/c)^2})/\sqrt{2} & (1,0) \text{ spiral}, \\ \sqrt{2+16(T/c)^2} & (1,1) \text{ spiral}, \\ \sqrt{2+8(T/c)^2} & (1,i) \text{ spiral}. \end{cases} \quad (\text{B5})$$

Each of the sums in Eqs. (4.11)–(4.13) is computed (in terms of dimensionless scaled variables) as a function of  $T/c$ . Each sum has a Bose-condensed piece corresponding to the  $k$ -vector  $\mathbf{k}_t$ . The equations are solved sequentially. Equation (4.11) determines the Bose-condensed fraction. The Bose-condensed parts of Eqs. (4.12) and (4.13) are then completely determined by the form of the numerator in the integrand. Equation (4.12) then gives the spin wave velocity (equivalently  $Q$ ) directly. Substituting this  $Q$  into Eq. (4.13) then determines  $F$ . Finally Eq. (4.14) or (B2) gives  $T/c$  in terms of  $\delta$ , so that the solution is obtained as a function of  $\delta$ . The free energies are then computed through Eq. (B3). We have carried out this procedure to order  $(T/c)^2$  (in  $E^{\text{MF}}$ ) for the

(1,0) and (1,1) spirals. The (1, $i$ ) spiral has a cusp singularity at  $T=0$  which we did not attempt to fit to any specified order. Rather, we solved the mean-field equations numerically for a range of small  $\delta$ :  $0.05(J/t) \leq \delta \leq 0.25(J/t)$ .

The full expression for the mean-field energy is

$$E^{\text{MF}} = -4JZ_c^2 S^2 + Z_1 4JS^2 \delta + \frac{1}{2} \kappa \delta^2, \quad (\text{B6})$$

$$Z_c = 1 + 0.078974/S,$$

$$Z_1 = Z_c^2 \left[ \left( 1 + \frac{1}{S} \right) - \frac{dZ_c}{dS} \right],$$

$Z_c$  is the spin wave velocity renormalization.<sup>9</sup>

For the (1,0) and (1,1) spirals, our numerical procedure provides an analytic expression for the compressibility  $\kappa(S, J, t)$  as follows:

$$\kappa(S) = -2JS^2 \left[ \left( \frac{t}{J} \right)^2 A(S) + \frac{4}{S} Z_c + \frac{1}{S^2} \right]. \quad (\text{B7})$$

Here

$$A(S) = \begin{cases} \left[ \frac{4}{S^2} \right] \frac{0.36 + 1.6(2S + 1 - 1.39)}{0.39 + 0.71(2S + 1 - 1.39)} & (1,0) \text{ spiral}, \\ \left[ \frac{16}{S^2} \right] \frac{0.57 + 0.01(2S + 1 - 1.39)}{0.39 + 0.71(2S + 1 - 1.39)} & (1,1) \text{ spiral}. \end{cases} \quad (\text{B8})$$

For  $S = \frac{1}{2}$ , we find that  $4Z_c^2 = 5.36$ , and  $4Z_1 = 14.36$ , while

$$\kappa_{1/2} = \begin{cases} +25.76 & (1,0) \text{ spiral}, \\ +44.16 & (1,1) \text{ spiral} \\ +0.99 & (1,i) \text{ spiral}, \end{cases} \quad (\text{B9})$$

Thus the (1,1) spiral wins.

The curvature of  $E^{\text{MF}}$  stays negative for all values of  $t/J$  and  $S$ . Although the (1,1) spiral has lower energy (due to the larger negative curvature) for small  $S$ , the

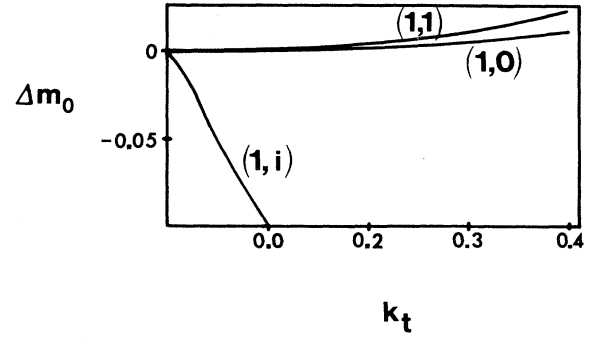


FIG. 4. The change in ground state staggered magnetization as a function of the pitch  $k_t$  for three symmetries of the spiral states. We see that the long-range order *increases* for the (1,0) and (1,1) twist, due to a reduction in the zero point quantum fluctuations.

(1,0) spiral is selected for  $S > 0.81$ .

In Fig. 4 we show the staggered magnetization  $m_0$  (one half of the Bose-condensed fraction) as a function of  $k_t$  for the three candidate spirals. For the (1,0) and (1,1) spirals, these are plots of the function

$$m_0(k_t) = (2S + 1 - \delta - 0.195) - \frac{\alpha}{16} \tan^2 k_t, \quad (\text{B10})$$

where  $\alpha$  is a numerical quantity proportional to the curvature of the integral (as a function of  $T/c$ ) computed for the left-hand side of Eq. (4.11), and equal to  $-1.0$  for the (1,0) spiral and  $-2.0$  for the (1,1) spiral. As Eq. (B10) makes clear, the dependence on  $S$  is trivial, for any of the spirals. Therefore we have plotted the *difference*  $\Delta m_0 = m_0(k_t) - m_0(0)$ , which is independent of  $S$ . For the (1, $i$ ) spiral,  $m_0$  is again computed graphically for small values of  $T/c$ .

When  $\delta=0$  then  $k_t=0$  and (B10) reproduces the known SBMFT result. Imposing a (1,0) or (1,1) spiral *increases*  $m_0$ . For the double spiral, which cannot be realized classically, the opposite result obtains as  $m_0$  is reduced by the enhanced quantum fluctuations.

<sup>1</sup>S. Chakravarty, in *Proceedings of the 1989 Los Alamos Symposium on High- $T_c$  Superconductivity*, Redwood City, CA, 1989, edited by K. S. Bedell, D. Coffey, D. Meltzer, D. Pines, and J. R. Schrieffer (Addison-Wesley, New York, 1990).

<sup>2</sup>R. R. P. Singh, Phys. Rev. B **39**, 9760 (1989).

<sup>3</sup>R. R. P. Singh and D. A. Huse, Phys. Rev. B **40**, 7247 (1989).

<sup>4</sup>J. D. Reger and A. P. Young, Phys. Rev. B **37**, 5978 (1988).

<sup>5</sup>Y. Okabe and M. Kikuchi, J. Phys. Soc. Jpn. **57**, 3451 (1988);

<sup>6</sup>T. Oguchi, Phys. Rev. **117**, 117 (1960).

<sup>7</sup>S. Chakravarty, B. I. Halperin, and D. R. Nelson, Phys. Rev. B **39**, 7443 (1988).

<sup>8</sup>D. P. Arovas and A. Auerbach, Phys. Rev. B **38**, 316 (1988).

<sup>9</sup>A. Auerbach and D. P. Arovas, Phys. Rev. Lett. **61**, 617 (1988).

<sup>10</sup>J. E. Hirsch and S. Tang, Phys. Rev. B **40**, 4769 (1989).

<sup>11</sup>C.-X. Chen and H. B. Schuttler, Phys. Rev. B **40**, 239 (1989).

<sup>12</sup>N. Read and S. Sachdev, Phys. Rev. Lett. **62**, 1694 (1989).

This paper provides a unified picture of the large- $N$  and large- $S$  approaches in the continuum (long-wavelength) limit.

<sup>13</sup>A. Auerbach and D. P. Arovas, J. Appl. Phys. **67**, 5734, (1990).

<sup>14</sup>W. Marshall, Proc. R. Soc. London, Ser. A **232**, 48 (1955).

<sup>15</sup>G. Baskaran, Z. Zou, and P. W. Anderson, Solid State Commun. **63**, 973, (1987).

<sup>16</sup>I. Affleck and J. B. Marston, Phys. Rev. B **37**, 3774 (1988).

<sup>17</sup>We thank Michael Ma for bringing this fact to our attention.

<sup>18</sup>S. Liang (unpublished).

<sup>19</sup>P. B. Visscher, Phys. Rev. B **10**, 943 (1974).

<sup>20</sup>L. B. Ioffe and A. I. Larkin, Phys. Rev. B **37**, 5730 (1988).

<sup>21</sup>V. J. Emery, S. A. Kivelson, and H. Q. Lin, Phys. Rev. Lett. **64**, 475 (1990).

<sup>22</sup>M. Marder, N. Papanicolaou, and G. C. Psaltakis, Phys. Rev. B **41**, 6920 (1990).

- <sup>23</sup>B. Schraiman and E. Siggia, Phys. Rev. Lett. **62**, 1564 (1989).
- <sup>24</sup>C. Jayprakash, H. R. Krishnamurthy, and S. Sarker, Phys. Rev. B **40**, 2610 (1989).
- <sup>25</sup>C. L. Kane, P. A. Lee, T. K. Ng, B. Chakraborty, and N. Read, Phys. Rev. B **41**, 2653 (1990);
- <sup>26</sup>B. Chakraborty, N. Read, C. Kane, and P. A. Lee, Phys. Rev. B **42**, 4819 (1990).
- <sup>27</sup>D. Yoshioka, J. Phys. Soc. Jpn. **58**, 1516 (1989).
- <sup>28</sup>In Ref. 25 after Eq. (4), the twist order parameter  $M_{\mathbf{k}}$  includes a component due to a ferromagnetic decoupling of the Heisenberg interaction.
- <sup>29</sup>M. F. Hundley, J. D. Thompson, S. W. Cheong, Z. Fisk, and J. E. Schirber, Phys. Rev. B **41**, 4062 (1990).
- <sup>30</sup>A. Aharony, R. J. Birgeneau, A. Coniglio, M. A. Kastner, and H. E. Stanley, Phys. Rev. Lett. **60**, 1330 (1988).
- <sup>31</sup>A. Auerbach and B. E. Larson (unpublished).
- <sup>32</sup>N. Read and D. M. Newns, J. Phys. C **16**, 3273, (1983).
- <sup>33</sup>Chakraborty *et al.* (Ref. 26) have suggested the possibility of nontrivial phases for the fields  $Q, K$ , which corresponds to noncoplanar spin configurations. In the long-range ordered phase, however, the spin energy increases linearly with the flux [A. Auerbach, B. Larson, and G. Murthy, Phys. Rev. B (to be published)], and we have found that it cannot be stabilized by the reduction of the fermion energy.
- <sup>34</sup>C. L. Kane, P. A. Lee, and N. Read, Phys. Rev. B **39**, 6880 (1989).
- <sup>35</sup>S. Sarker, C. Jayprakash, H. R. Krishnamurthy, and M. Ma, Phys. Rev. B **40**, 5028 (1989).
- <sup>36</sup>P. B. Wiegmann, Phys. Rev. Lett. **60**, 821 (1988).
- <sup>37</sup>X.-G. Wen Phys. Rev. B **39**, 7223 (1989).
- <sup>38</sup>P. A. Lee, Phys. Rev. Lett. **63**, 690 (1989).